Journal Name

ARTICLE

Inelastic behaviour of cellulose microfibril networks

Srivatssan Mohan [a]*, Gijsje H. Koenderink [b] and Krassimir P. Velikov [a,c,d]*

Received 00th January 20xx,
Accepted 00th January 20xx

DOI: 10.1039/x0xx00000x

www.rsc.org/

Cellulose microfibrils (CMF) are a unique class of shape anisotropic bio-nanomaterials, already finding many applications in diverse fields owing to their advantageous material properties and abundant availability. The rich non-linear mechanical behaviour of CMF networks has been under-studied due to the complex nature of this system, being influenced by many factors such as strong inter-fibril interactions, a heterogeneous microstructure, and process conditions. In this work, we systematically explore the non-linear rheological behaviour of these networks using a CMF model system with controlled process conditions and fibril interactions. The microfibrils were dispersed in dimethyl sulfoxide to minimise the attractive van der Waals interactions and thereby also the network heterogeneity. We show that the networks exhibit a transition with increasing shear stress from a predominantly elastic to a plastic deformation where they undergo softening. We find that the network stiffness and plasticity are dependent on the loading rate. Finally, we observed that the networks regain their original viscoelastic moduli on cessation of shear. These findings form a basis towards understanding and ultimately modelling the mechanics of CMF networks, which is a prerequisite for the rational design of novel bio-based materials.

Introduction

Cellulose microfibrils (CMF), also known as nanocellulose or cellulose nanofibrils,[1,2] are amongst the most fascinating fibrillar biopolymer systems. In addition to their critical function in the mechanical reinforcement of tissues of plants, CMFs are also widely used in industrial applications ranging from food products to high strength composites.[3-7] Research on cellulosic materials therefore comprises a significant part of current renewable and sustainable materials research. CMF networks have the advantage that they can be fabricated into many different forms such as films, aerogels, hydrogels, dispersions and composites, depending on the requirements of the application.[5,8-10]

Understanding the mechanical properties of CMFs and the networks they form holds the key to effectively exploit their potential. The mechanical properties of single fibrils are relatively well-characterized. CMF have been shown to exhibit rather unique mechanical properties, having a large length/diameter (aspect ratio) and a remarkably high elastic modulus compared to other biopolymers.[11,12] In suspension, the CMFs can either form an isotropic or an anisotropic network structure depending on their dominant interactions, surface chemistry and processing conditions.[13,14] The resulting network structure in turn influences the mechanical response of the networks. Accordingly, the emergent macroscopic behaviour of the networks formed by CMFs is complex and poorly understood, being the result of a net effect of different factors such as single-fibril properties, inter-fibril interactions, process conditions, and the network micro-structure. Some of the universal rheological characteristics of CMF networks reported include gel-like behaviour at low concentrations, shear thinning and thixotropic effects (reviewed in [15,16]). The study of the rheological properties of CMF networks, especially in aqueous media, however, is impaired due to the complex flow behaviour of the particles arising from their large aspect ratio and strong inter-particle interactions, causing flocculation and bundling of the fibrils. This leads to depletion of particles in the vicinity of the surface of the measuring geometry of the rheometer (i.e. wall-slip) and non-uniform flow profiles causing shear banding.[15,17,18]

Owing to the aforementioned issues, the rheological properties of CMF networks, especially in the nonlinear regime, are not well characterized and much less well understood than the mechanics of other biopolymer networks, such as fibrin, collagen and actin networks.[19]

[a] *Soft Condensed Matter, Debye Institute for NanoMaterials Science, Utrecht University, Princetonplein 5, 3584 CC Utrecht, The Netherlands.*
[b] *AMOLF, Living Matter Department, Science Park 104, 1098 XG Amsterdam, The Netherlands.*
[c] *Unilever R&D Vlaardingen, Olivier van Noortlaan 120, 3133 AT Vlaardingen, The Netherlands.*
[d] *Institute of Physics, University of Amsterdam, Science Park 904, 1018 XH Amsterdam, The Netherlands.*

Electronic Supplementary Information (ESI) available: Comparison of different geometries for wall-slip effects, determination of fractal dimensions of single CMFs and the results of cyclic constant maximum strain cycles.
See DOI: 10.1039/x0xx00000x

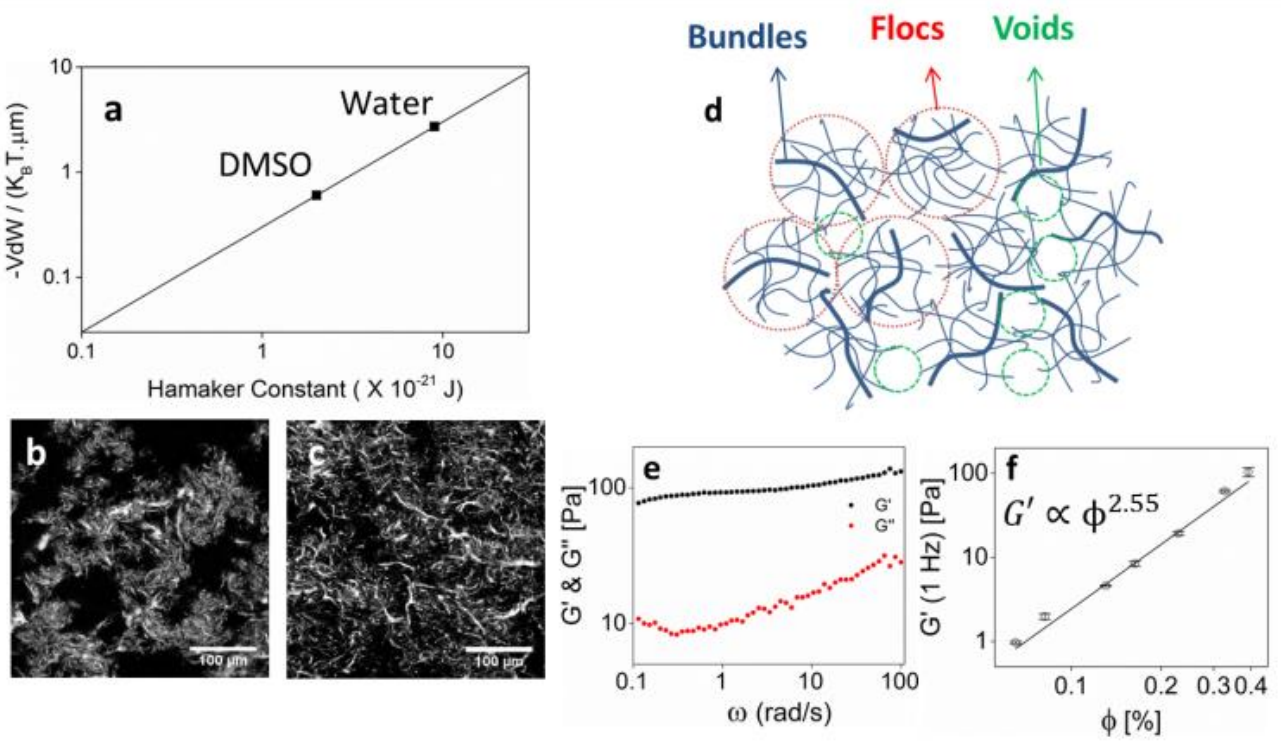

Fig.1: (a) Average Van der Waals attraction energy between a pair of CMFs oriented in parallel, separated by a 30 nm distance, calculated assuming a cylindrical shape for the fibril cross-section. (b) 2D confocal fluorescence image of CMF networks at a volume fraction of 0.33% in water clearly show the presence of a larger area of voids in comparison to (c) the corresponding networks in DMSO. (d) Schematic illustration of the heterogeneous microstructure of CMF dispersions comprising bundles, flocs and voids. (e) Representative linear viscoelastic frequency spectrum of a 0.33% CMF dispersion in DMSO at 0.1% imposed oscillatory strain. (f) Dependence of the storage modulus of the networks on the fibril volume fraction, together with a power law fit with an exponent of 2.55 ± 0.12.

Here we aim to explore the mechanical behavior of CMF networks in response to large shear deformations. To elucidate the intrinsic mechanical response of CMF networks, we use CMF produced by bacteria (average cross-sectional dimension of 60 × 5 nm and up to several micrometers in length),[20] which unlike other CMF sources can be produced without markedly altering the surface chemistry or mixing with dispersing agents.[1,2] We process the fibrils dispersed in solvents with a low dielectric constant, using an industrially relevant ultra-high-energy mechanical deagglomeration method. This method leads to the formation of CMF networks that are substantially less heterogeneous than the networks that are typically formed in water.[21,22] We use shear rheometry supplemented by confocal microscopy to study the mechanical response and relate this to the underlying microstructure of the networks. We show that the fibril networks undergo a transition with increasing shear stress from a predominantly elastic to a plastic deformation and are capable of quickly regaining their original viscoelastic moduli upon removal of the stress.

Experimental

The bacterial cellulose microfibrils (CMF) were sourced from a commercial Nata de coco product (Cozzo Food Industries, Malaysia). The CMFs were fluorescently labelled by covalent modification with fluorescein isothiocyanate (≥90%, Sigma-Aldrich) and processed once using a Microfluidizer™ M-110S (Microfluidics Corp), operated at a pressure of 1200 bar. The details of the dispersion preparation procedure of CMFs in dimethyl sulfoxide (DMSO) (≥99.9% ACS reagent, refractive index n_D^{20} 1.479, Sigma-Aldrich) are described in our previous work.[23] Samples at different volume fractions ϕ were made by concentrating the stock dispersion by centrifugation (except for the 0.06% and 0.08% samples) at 3566 g (Hettich ROTANTA 460R) for 20 mins using 50 mL conical-bottom centrifuge tubes, taking into account the mass density of CMF as 1.5 g/mL.[24] After centrifugation, a certain amount of supernatant was removed using a pipette to attain a specific volume fraction and the concentrated dispersion was re-homogenized by mixing in a universal small shaker at 2500 RPM. The dilute samples (0.06% and 0.08%) were prepared by diluting the stock dispersion with DMSO, followed by mixing in a universal small shaker at 2500 RPM.

Small amplitude oscillatory shear and rotational shear rheology measurements were performed using stress-controlled rheometers, either an MCR 302 or MCR 301 (Anton Paar, Graz, Austria) with a parallel plate geometry configuration (gap size= 0.80 mm). A sand-blasted stainless steel top plate (Ø= 50 mm) was used. We chose a parallel plate geometry despite the disadvantage of an inhomogeneous shear rate since the gap size of this system is adjustable and we could thus avoid localization of our high aspect ratio particles. The availability of a sand-blasted measuring plate in

this configuration is further useful to minimize the occurrence of wall-slip effects. The samples were carefully transferred to the rheometer bottom plate with a plastic spoon and all the measurements were done at a constant temperature of 22°C maintained by a Peltier plate. The measurements were started after resting the sample for five minutes upon lowering the top plate. No pre-shear process was applied in order to not change the sample structure. To confirm the absence of wall-slip effects in the measurements, we checked that no changes in the strain response occurred in response to rotational stress ramps at different gap sizes ranging from 0.5 to 1.2 mm (Fig. S1). Confocal fluorescence microscopy was performed using a Leica TCS SP8 microscope with a 40 × NA 1.3 oil immersion objective (n_D^{20}=1.515). The samples were illuminated at 495 nm and recorded in a 512 × 512 pixel format.

Results and discussion

It is known that native CMFs, when dispersed in water, associate and form networks with a heterogeneous microstructure comprising fibril bundles, flocs and voids owing to attractive van der Waals and hydrogen bonding interactions.[22, 25] This heterogeneous microstructure can lead to complications in the rheological response of CMF dispersions such as wall slip and shear banding.[17,18] We hypothesized that the attractive interactions, dominated by van der Waals forces between the fibrils, can be reduced by dispersing the fibrils in a lower dielectric constant medium and thus lowering the effective Hamaker constant. To test this, we dispersed CMFs in dimethyl sulfoxide (DMSO), which has a smaller dielectric contrast with cellulose ($\varepsilon_{DMSO} - \varepsilon_{Cellulose}$ = 46.68 – 7 = 39.68) compared to water ($\varepsilon_{Water} - \varepsilon_{Cellulose}$ = 80.10 – 7 = 73.1).[26, 27] The Hamaker constants were calculated by using Lifshitz theory,[28] employing the isotropic refractive index value of CMF as 1.569.[29] The van der Waals interaction between a parallel pair of CMFs was calculated assuming a cylindrical shape of the fibril cross-section.[30] We calculated that the van der Waals interactions between CMFs in DMSO should be about four times lower than in water (Fig. 1a). Consistent with our hypothesis, confocal imaging qualitatively confirmed that CMF networks dispersed in DMSO were significantly less heterogeneous than networks in water (Fig. 1b, c), although we still observed bundles, flocs and voids (see schematic in Fig. 1d).

To characterize the linear viscoelastic behavior of the CMF dispersions in DMSO, we performed small amplitude oscillatory measurements over a frequency (ω) range from 0.1 to 100 rads/s. The frequency sweep was performed at a constant strain amplitude of 0.1%, within the linear viscoelastic regime (~1% strain), which was determined from amplitude sweep measurements. As shown in Fig. 1e, the storage modulus (G') was higher than the loss modulus (G'') over the entire frequency range, indicating a predominantly elastic response. There is a slight power law dependence of the storage modulus on frequency with an exponent of 0.07, which is characteristic of gels held together by weak physical crosslinks and consistent with prior measurements on bacterial cellulose (BC) networks in water.[31] The physical gel-like state of the networks is also reflected in the minimum of the loss modulus at a frequency of 0.3 rad/s. This characteristic frequency indicates a transition of the viscoelastic response from being dominated by a transient to a static state of the crosslinks between fibrils.[32]

The storage modulus at a fixed strain oscillation frequency (6.28 rad/s or 1 Hz) increases with CMF volume fraction as a power-law in the range of 0.06% to 0.50% (Fig. 1f). In this volume fraction range, the network did not show any collapse or sedimentation with time, indicating connectivity percolation. Theoretically, the percolation threshold (ϕ_c) of thin hard rods based on the average diameter (D) and length (L), assuming that the number of contacts per rod (α) equals unity, is given by the expression, $\phi_c \sim \alpha D/L \geq 0.2\%$.[33] The experimentally observed smaller percolation value of ≤ 0.06% can be attributed to the attractive interactions between the particles, which is known to lower the percolation threshold.[34] The best fit power law exponent characterizing the concentration dependence of the storage modulus is 2.55 ± 0.12. Prior studies of different types of CMF networks have reported a wide range of concentration exponents from 2 to 5.2.[15] This variability is likely due to the structural heterogeneity of CMF networks. In the absence of heterogeneities, we would expect an exponent of 2.0 according to theoretical models of networks of rigid rods (fractal dimension, D_F = 1) wherein bending deformations are predominant with frozen junctions.[35-37] From image analysis of individual fibrils, we indeed found that D_F is close to unity for the CMFs (Fig. S2). Furthermore, the thermal persistence length of the fibrils, $l_p = E.I/k_B.T$, is expected to be of order 12 mm given a Young's modulus (E) of 78 GPa for cellulose[11] and taking the second moment of inertia (I) based on an average width and height of the fibril cross-section as 60 nm and 5 nm,[20] respectively. This estimated persistence length is

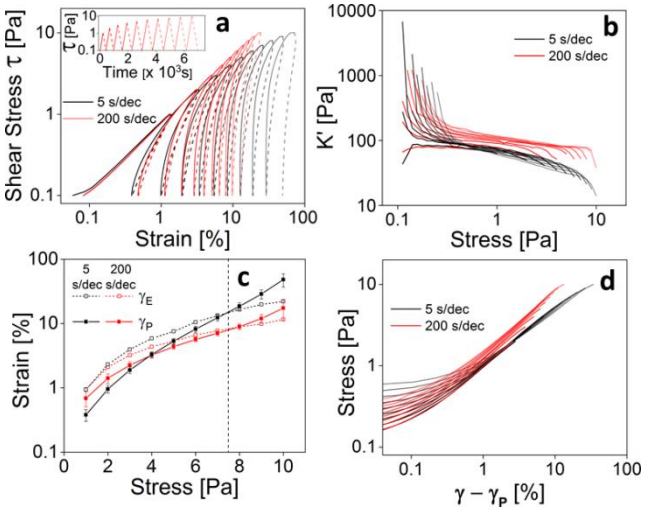

Fig. 2 (a) Stress-strain plot of CMF dispersion (ϕ= 0.33%) in DMSO on application of consecutive stress ramp cycles with increasing maximum stress, at two different rates; the solid and dashed lines represent the loading and unloading parts, respectively of a cycle. Inset: The input stress ramps at a constant logarithmic rate of 200 s/decade. (b) Differential elastic modulus obtained from the loading curves in (a), showing stress softening. (c) The evolution of γ_P and γ_E with every stress cycle, showing a crossover as marked by the vertical dashed line. (d) Rescaled stress-strain plots obtained by subtracting off γ_P from the total strain for the loading part of the curves.

much greater than the average length of the fibrils; therefore CMFs can be classified as stiff rod-like particles. Due to the shape anisotropy of the fibril cross-section and twists inherent in the CMFs, the determination of the true persistence length can be challenging and can often lead to its under-estimation by image analysis methods.[38]

In order to study the non-linear rheological properties of CMF networks, we first performed rotational shear rheology measurements comprising stress ramp cycles consisting of first increasing and then decreasing stress ramps with increasing maximum stress (inset of Fig. 2a). Fig. 2a shows the stress-strain response for a CMF network with a volume fraction of 0.33% with increasing maximum stress cycles at two different logarithmic rates. We first consider the derivative of the upward part of the stress-strain curves, which corresponds to the differential elastic modulus (K'). As shown in Fig. 2b, the differential modulus curves obtained in subsequent stress ramps almost converge and show a decreasing trend as a function of applied stress. These trends are similar for both loading rates, but with a higher elastic modulus at the slower rate. We conclude that CMF networks undergo stress softening.

Going back to Fig. 2a, we observe that the decreasing cycle is different from the increasing one, and there is a residual strain (γ_P) at the end of every cycle, which increases with each subsequent cycle. This instantaneous value of the strain at the end of every cycle corresponds to the plastic deformation undergone by the network. The difference between the strain at maximum stress and the residual strain is the recovered strain (γ_E), or the elastic component of the deformation. We find that at both loading rates, γ_E is initially higher than γ_P, and increases with the applied maximum stress until the stress reaches about 8 Pa, after which γ_P predominates (Fig. 2c). Therefore, the deformation is predominantly elastic until a certain value of applied stress, after which plastic deformation takes over. When the γ_P value of the preceding cycle is subtracted from the increasing ramps, the set of curves obtained at each loading rate almost collapse onto a single master curve, as depicted in Fig. 2d. This observation reinforces the stress softening nature of the networks.

Theoretical models of rigid rod networks typically predict a strain-stiffening response due to shear-induced fibril alignment and a transition from a soft, bending-dominated elastic regime at small strains to a rigid, stretching-dominated elastic regime at large strains.[36,39] For CMFs, bending may potentially be further favored by weak regions such as twists in the fibrils, which are spaced at the same length scale as the network mesh size.[23] However, these models assume permanent crosslinks. For biopolymer networks like fibrin and collagen the crosslinks between fibrils are indeed nearly permanent, and the networks strain-stiffen.[40, 41] In contrast, the CMFs interact via transient, noncovalent interactions. The stress-softening response of the CMF networks suggests that shear induces dissociation of these transient crosslinks. On stress reversal, the fibrils can quickly reform junctions, thereby regaining their initial elastic modulus. The observation that K' is higher at the slower loading rate suggests that the weak physical crosslinks between the fibrils have more time to re-bind and form a stiffer network conformation at slower loading rates.

To verify whether the network response changes when subjected to repeated stress cycles in the predominantly plastic regime, we subjected the samples to repeated stress cycles with a constant maximum stress of 8 Pa, again comparing two different loading rates (Fig. 3a inset). The strain response to the imposed constant stress cycles was similar for both loading rates, exhibiting a residual deformation at the end of every cycle as displayed in Fig. 3a. The differential

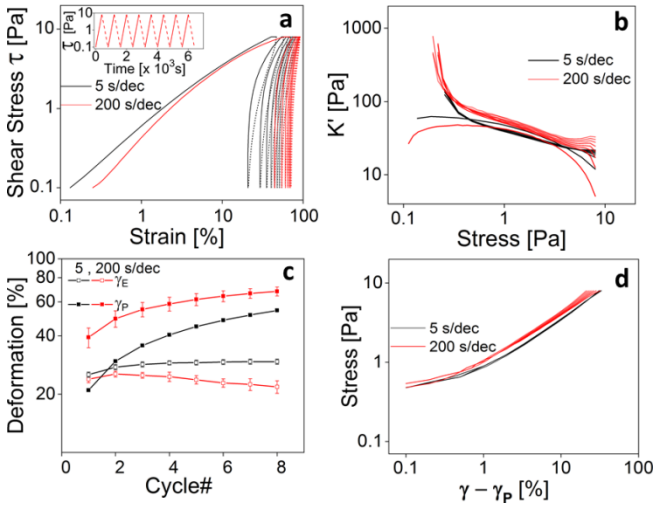

Fig. 3 (a) Evolution of strain of CMF sample (ϕ= 0.33%) with application of repeated constant stress cycles going up to a maximum stress of 8 Pa. Inset: Input stress cycles at a fixed logarithmic rate of 200 s/decade. (b) Differential elastic modulus plotted against the applied stress with an overlay of all the cycles, (c) Evolution of γ_E and γ_P with the applied stress cycles. (d) Rescaled stress-strain curves of the loading portions of the stress cycles obtained by subtracting off the residual strain from the total strain.

elastic modulus obtained by taking a derivative of the upward (loading) part of the stress cycles again shows stress softening, resembling the trend we observed in the first set of cyclic measurements where we increased the maximum stress (Fig. 3b). Also consistent with those measurements, we observe that γ_P is higher than γ_E for all the cycles, except for the first cycle at the faster loading rate (Fig. 3c). We find that γ_P increases with each subsequent cycle but it appears to saturate after ~8 cycles. Interestingly, γ_E is only weakly dependent on the number of stress cycles. Repeated stress ramps for a constant maximum stress of 8 Pa again collapse onto a single master curve when γ_P of every preceding cycle is subtracted off from the total strain, as shown in Fig. 3d. In short, the inelastic behaviour persists, yet the stress softening

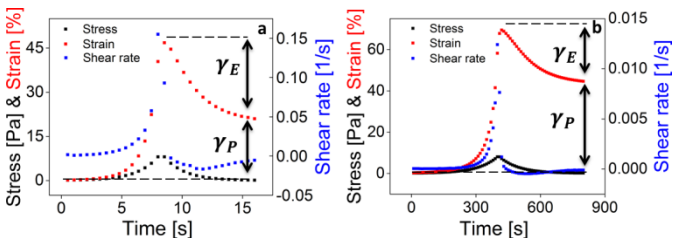

Fig. 4 Evolution of strain and shear rate along with the applied stress cycle (8 Pa) as a function of time at (a) 5 s/dec (b) 200 s/dec.

phenomenon does not change despite the networks undergoing a predominantly plastic deformation. In order to verify that the recorded behaviour of CMF networks is not an artefact of the measuring system used, we performed the same tests with a cone-plate geometry, which has the advantage of a homogeneous shear rate through the sample. A qualitatively similar behaviour to the plate-plate configuration was observed, in which the networks show an increasing degree of plastic deformation with applied stress cycles (Fig. S3).

The effect of the applied stress rate on the plastic and elastic deformation incurred on CMF networks is apparent from Fig. 4, which shows the evolution of strain and shear rate with time on application of a single stress cycle (first cycle in Fig. 3a). These graphs confirm that the measurements were done in non-steady state conditions.

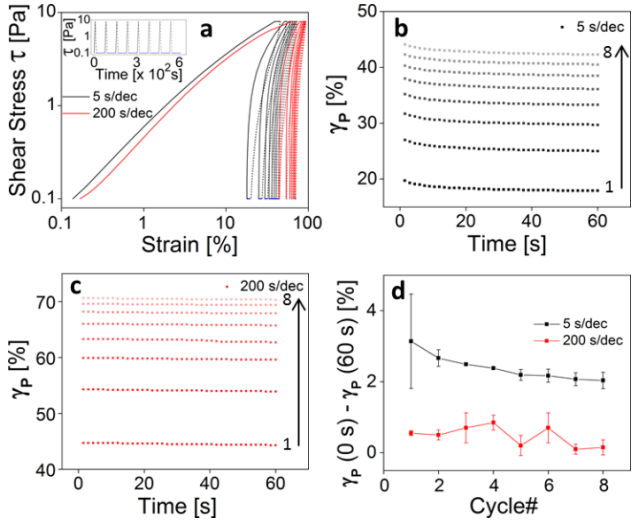

Fig. 5 (a) Evolution of strain with application of constant stress cycles of 8 Pa with intermediate pauses of 60 s on ϕ= 0.33% CMF. Inset: Stress input at a fixed rate, the blue lines at a constant stress of 0.1 Pa denote the pauses between the stress cycles. (b, c) Relaxation of the residual strain during the 60 s pause interval for the faster and slower rate of applied stress, respectively. (d) The change in γ_P during the pause interval as a function of stress cycles for both loading rates.

Finally, we measure the inelastic response when the stress is held constant at 0.1 Pa for 60 s in between every cycle, with the aim to test whether or not γ_P is transient. Again, we observe markedly inelastic behavior (Fig. 5a). We observe a slight decrease of γ_P with pause time for the faster loading rate (Fig. 5b), but virtually no change in γ_P with time for the slower loading rate (Fig. 5c). Figure 5d shows a direct comparison of the strain recovered during the 60 s waiting time for the two rates, which amounts to ~3% for the faster rate and only 0.5% for the slower rate. The recovery of γ_P likely occurs due to the reformation of fibril cross-links with time, revealing that the induced deformations are recoverable, depending on the rate of applied stress. For the faster rate, γ_P decreases with the number of cycles, which shows the influence of the sample shear history on the mechanical response (Fig. 5d).

To further investigate the recovery behaviour of CMF networks, a stress pulse experiment was conducted. A short

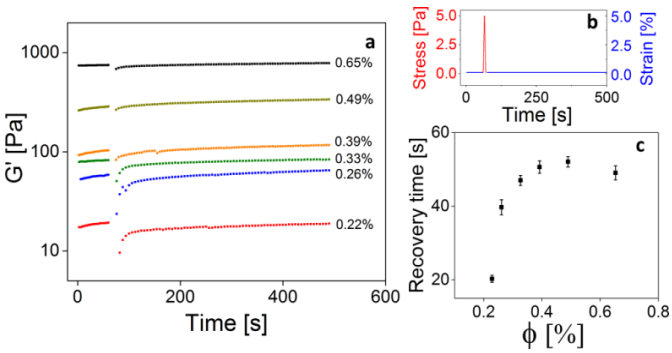

Fig. 6 (a) The evolution of G' after a stress pulse (see panel b) as a function of time monitored by small amplitude oscillatory shear strain measurements for different volume fractions of CMF. (c) The recovery times of CMF networks in response to a stress pulse of 5 Pa at different volume fractions.

stress pulse was applied to disrupt the structure of the sample amidst a small amplitude oscillatory time sweep, as shown in Fig. 6b. We monitor the evolution of G' after the stress pulse as a proxy of the recovery of the sample structure after the damage (Fig. 6a). The recovery curves are well-fitted by an exponential function, as described by Wolff *et al.*,[42] (normalized for the G' drift with time), providing an estimate of the recovery time of the networks. The recovery time initially increases from 20 s to 52 s with increasing CMF volume fraction and saturates above volume fractions of 0.4 % for the applied stress of 5 Pa (Fig. 6c). At high fibril volume fractions above 0.4%, the increasing elastic modulus of the networks probably compensates the damage incurred, as the resulting deformation inflicted by the same applied stress is smaller. Our findings are consistent with earlier work of Naderi *et al.*, who also reported that CMF networks in water, irrespective of their surface chemistry, rapidly regain their rheological properties on cessation of shear.[43]

In order to study the response of the CMF networks close to failure and the softening limit, we performed linear strain ramp cycles with increasing (and decreasing) maximum strain (Fig. 7a) and constant maximum strain (Fig. S4). Interestingly, we observe that a negative value of stress was required to restore the strain value back to zero, at the end of every cycle (Fig. 7c). In addition, we observe a significant difference in the stress response between the increasing and decreasing maximum strain cycles. In the case of decreasing maximum strain cycles, there is a large hysteresis in the first cycle followed by a large drop (by more than three-fold) in the hysteresis loop area in the subsequent cycles. This hysteresis loop area corresponds to the energy dissipated per strain cycle due to both network rearrangements (un-binding and re-binding of physical cross-links) and other viscous effects. Carbon nanotube networks are also known to show a similar dissipation behaviour due to reversible zipping and un-zipping of the nanotubes under cyclic strain.[44] In the case of increasing maximum strain, the network remodeling occurs steadily with every cycle and at the last cycle (100 % strain), the dissipation energy value is still lower than the first decreasing maximum strain cycle; affirming the influence of shear history on the mechanical response of these networks (Fig. 7b). The stress

(τ_{max}) at the maximum applied strain and back at zero strain (τ_{min}) at the end of every cycle is plotted as a function of the

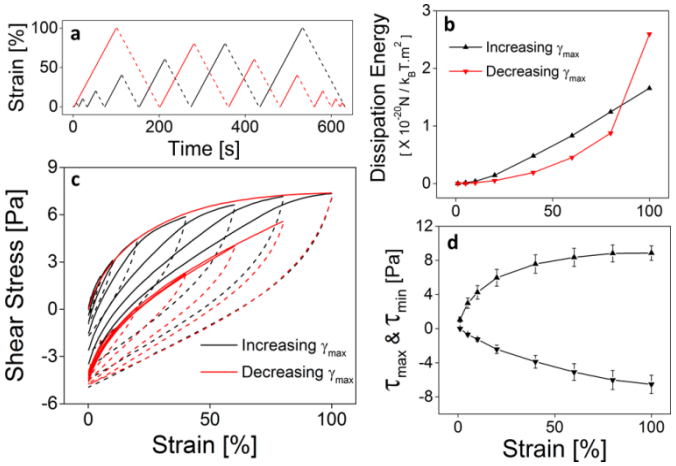

Fig. 7 (a) Linear strain ramp experiment protocol at a strain rate of 1%/s with increasing and decreasing maximum strain. (b) The dissipation energy (normalized to k_BT) plotted against the applied maximum strain cycle based on the (c) Stress response of CMF network (ϕ= 0.33%) to the strain cycles at 1%/s. (d) The maximum (▲) and minimum (▼) stress attained as a result of increasing maximum strain cycles.

applied cycles in Fig. 7d. Both τ_{max} and τ_{min} initially increase with increasing applied strain and then reach a plateau, which indicates cessation of network remodeling i.e. the onset of fatigue, eventually leading to network failure. On applying repeated strain cycles with a constant maximum strain, τ_{max} decreases and τ_{min} recovers with the number of cycles (Fig. S4a-d). The dissipation energy drops markedly after the first cycle (Fig. S4e). Altogether, this indicates that the network softens dynamically, without any signs of failure, due to the fast reformation of physical cross-links. Thus, the mechanical integrity of the networks is retained. However, the faster the application of strain, the less the network remodels and the sooner the material approaches fatigue (Fig. S4c-d).

Conclusions

We showed that CMF networks dispersed in a low dielectric medium solvent are predominantly elastic at small strains, with a characteristic power-law scaling of G' with volume fraction. In the non-linear regime, we observed a marked inelastic response. The networks exhibit stress-softening and they undergo a transition from a predominantly elastic to a plastic deformation with increasing shear stress. The loading rate also influences the mechanical response of the networks, as evidenced by a higher network stiffness at the slower loading rates (increasing stress cycles) and in differences in the induced residual deformation (constant stress cycles with pauses). From the cyclic strain experiments, we detected dynamic softening and discovered that the CMF networks respond differently based on the shear history of the system. Interestingly, the CMF networks did not show any symptoms of failure to the applied constant maximum strain cycles at slower rates, which can be attributed to the reformation of cross-links in the network. We also found that the networks were quickly able to regain their original properties by the re-formation of the weak physical cross-links after a deformation event, which reveals a reversible stress softening phenomenon.

The results provided in this study advance the understanding of the mechanics of athermal fibrillar networks and show how weak physical interactions can play an important role in shaping the nonlinear rheological response. The findings from this study can be applied towards designing bio-based shape-tunable materials by exploiting the mechanosensitivity of CMF networks.

Conflicts of interest

There are no conflicts to declare.

Acknowledgements

We thank Gideon van den Brink for the calculation of the van der Waals interaction between the fibrils and Roland Gouzy for his assistance in processing the CMF dispersions. This work is part of the research program of the Foundation for Fundamental Research on Matter (FOM) and was financially supported by a FOM program grant (Grant number 143). The work was also supported by DiStruc Marie Sklodowska Curie Innovative Training Network (Grant Agreement No.641839) and NanoNextNL (a consortium of the Dutch government and 130 other partners).

References

1. G. Chinga-Carrasco, *Nanoscale Res. Lett.*, 2011, **6**, 417.
2. D. Klemm, F. Kramer, S. Moritz, T. Lindström, M. Ankerfors, D. Gray and A. Dorris, *Angew. Chem. Int. Ed.*, 2011, **50**, 5438-5466.
3. H. Wei, K. Rodriguez, S. Renneckar and P. J. Vikesland, *Environ. Sci. Nano*, 2014, **1**, 302-316.
4. H. Jin, M. Kettunen, A. Laiho, H. Pynnönen, J. Paltakari, A. Marmur, O. Ikkala and R. H. A. Ras, *Langmuir*, 2011, **27**, 1930-1934.
5. C. Salas, T. Nypelö, C. Rodriguez-Abreu, C. Carrillo and O. J. Rojas, *Curr. Opin. Colloid Interface Sci.*, 2014, **19**, 383-396.
6. M. Frey, D. Widner, J. S. Segmehl, K. Casdorff, T. Keplinger and I. Burgert, *ACS Appl. Mater. Interfaces*, 2018, **10**, 5030-5037.
7. Z. Shi, Y. Zhang, G. O. Phillips and G. Yang, *Food Hydrocolloids*, 2014, **35**, 539-545.
8. K. J. De France, T. Hoare and E. D. Cranston, *Chem. Mat.*, 2017, **29**, 4609-4631.
9. M. A. Hubbe, A. Ferrer, P. Tyagi, Y. Yin, C. Salas, L. Pal and O. J. Rojas, *BioResources*, 2017, **12**, 2143-2233.
10. K.-Y. Lee, Y. Aitomäki, L. A. Berglund, K. Oksman and A. Bismarck, *Compos. Sci. Technol.*, 2014, **105**, 15-27.
11. G. Guhados, W. Wan and J. L. Hutter, *Langmuir*, 2005, **21**, 6642-6646.
12. S. Iwamoto, W. Kai, A. Isogai and T. Iwata, *Biomacromolecules*, 2009, **10**, 2571-2576.
13. F. Jiang, S. Han and Y.-L. Hsieh, *RSC Adv.*, 2013, **3**, 12366-12375.
14. M. Zhao, F. Ansari, M. Takeuchi, M. Shimizu, T. Saito, L. A. Berglund and A. Isogai, *Nanoscale Horiz.*, 2018, **3**, 28-34.
15. O. Nechyporchuk, M. N. Belgacem and F. Pignon, *Biomacromolecules*, 2016, **17**, 2311-2320.
16. A. Naderi, *Cellulose*, 2017, **24**, 1933-1945.

17. O. Nechyporchuk, M. N. Belgacem and F. Pignon, *Carbohydr. Polym.*, 2014, **112**, 432-439.
18. F. Martoia, C. Perge, P. J. J. Dumont, L. Orgeas, M. A. Fardin, S. Manneville and M. N. Belgacem, *Soft Matter*, 2015, **11**, 4742-4755.
19. F. Meng and E. M. Terentjev, *Soft Matter*, 2016, **12**, 6749-6756.
20. R. J. Moon, A. Martini, J. Nairn, J. Simonsen and J. Youngblood, *Chem. Soc. Rev.*, 2011, **40**, 3941-3994.
21. M. A. Hubbe and O. J. Rojas, *BioResources* 2008, **3**, 1419−1491.
22. A. Kuijk, R. Koppert, P. Versluis, G. van Dalen, C. Remijn, J. Hazekamp, J. Nijsse and K. P. Velikov, *Langmuir*, 2013, **29**, 14356-14360.
23. S. Mohan, J. Jose, A. Kuijk, S. J. Veen, A. van Blaaderen and K. P. Velikov, *ACS Omega*, 2017, **2**, 5019-5024.
24. C. Sun, *J. Pharm. Sci.*, 2005, **94**, 2132-2134.
25. S. M. Notley, B. Pettersson and L. Wågberg, *J. Am. Chem. Soc.*, 2004, **126**, 13930-13931.
26. R. A. Hovermale and P. G. Sears, *J. Phys. Chem.*, 1956, **60**, 1579-1580.
27. J. Brandrup, E. H. Immergut and E. A. Grulke, *Polymer Handbook, 4th Edition*, Wiley, New York, 1999.
28. J. N. Israelachvili, in *Intermolecular and Surface Forces (Third Edition)*, Academic Press, San Diego, 2011.
29. P. H. Hermans, *Contribution to the Physics of Cellulose Fibres*, Elsevier New York, 1946.
30. V. A. Parsegian, *Van der Waals Forces: A Handbook for Biologists, Chemists, Engineers, and Physicists*, Cambridge University Press, 2005.
31. F. G. Torres, O. P. Troncoso, D. Lopez, C. Grande and C. M. Gomez, *Soft Matter*, 2009, **5**, 4185-4190.
32. O. Lieleg, M. M. A. E. Claessens, Y. Luan and A. R. Bausch, *Phys. Rev. Lett.*, 2008, **101**, 108101.
33. A. P. Philipse, *Langmuir*, 1996, **12**, 1127-1133.
34. B. Vigolo, C. Coulon, M. Maugey, C. Zakri and P. Poulin, *Science*, 2005, **309**, 920.
35. J. L. Jones and C. M. Marques, *J. Phys. France*, 1990, **51**, 1113-1127.
36. A. J. Licup, S. Münster, A. Sharma, M. Sheinman, L. M. Jawerth, B. Fabry, D. A. Weitz and F. C. MacKintosh, *Proc. Nat. Acad. Sci.*, 2015, **112**, 9573-9578.
37. R. L. Satcher and C. F. Dewey, *Biophys. J.*, 1996, **71**, 109-118.
38. I. Usov, G. Nyström, J. Adamcik, S. Handschin, C. Schütz, A. Fall, L. Bergström and R. Mezzenga, *Nat. Comm.*, 2015, **6**, 7564.
39. A. Sharma, A. J. Licup, K. A. Jansen, R. Rens, M. Sheinman, G. H. Koenderink and F. C. MacKintosh, *Nat. Phy.*, 2016, **12**, 584.
40. Nicholas A. Kurniawan, Bart E. Vos, A. Biebricher, Gijs J. L. Wuite, Erwin J. G. Peterman and Gijsje H. Koenderink, *Biophys. J.*, 2016, **111**, 1026-1034.
41. S. Münster, L. M. Jawerth, B. A. Leslie, J. I. Weitz, B. Fabry and D. A. Weitz, *Proc. Nat. Acad. Sci.*, 2013, **110**, 12197-12202.
42. L. Wolff, P. Fernández and K. Kroy, *PLOS ONE*, 2012, **7**, e40063.
43. A. Naderi and T. Lindström, *NORD PULP PAP RES J*, 2016, **31**, 354-363.
44. M. Xu, D. N. Futaba, T. Yamada, M. Yumura and K. Hata, *Science*, 2010, **330**, 1364.

TOC

Weak physical interactions between cellulose microfibrils play an important role in shaping their nonlinear rheological response.